Supporting Information

NADH- Selective and Sensitive Fluorescence Probe for Evaluate Living Cell Hypoxic Stress

General spectroscopic methods

The reagents used in the organic synthesis and spectroscopic analysis were all commercially available analytically pure reagents and were used without further purification. 10 mM phosphate buffer (pH = 7.4), RMPI1640 medium, trypsin, fetal bovine serum, etc. were purchased from Tianjin Dingguo Biotechnology Co., Ltd. The water used in the spectral analysis is ultrapure water, no fluorescent impurities. NMR spectra were recorded on a Bruker spectrometer at 400 (^{1}H NMR) MHz and 100 (^{13}C NMR) MHz. Chemical shifts (δ values) were reported in ppm down field from internal Me_4Si (^{1}H and ^{13}C NMR). High-resolution mass spectra (HRMS) were acquired on an Agilent 6510 Q-TOF LC/MS instrument (Agilent Technologies, Palo Alto, CA) equipped with an electrospray ionization (ESI) source. Melting points were recorded on a melting point apparatus (RY-2, Tianjin, China). UV absorption spectra were done by a Shimadzu UV-2550 UV/Vis spectrophotometer with 1 cm quartz cell. Fluorescence emission spectra are obtained by a Hitachi F-4600 spectro-fluorophotometer with a 1 cm quartz cell. The pH values were reported by a Mettler Toledo SevenExcellence pH meter (Mettler Toledo MP 220, Shanghai, China). The absorbance for MTT analysis was recorded on a microplate reader (PL-9602, Beijing, China). The confocal microscopy imaging was used Olympus FV1000-IX81 inverted fluorescence microscope. All images were analyzed with Olympus FV1000-ASW.

Solution preparation

DPMQL1 were dissolved in DMSO to obtain 5×10^{-3} M stock solutions. Metal ions, ions, amino acids, reducing substances and oxidizing substances were dissolved in ultrapure water to obtain 1×10^{-2} M stock solutions, respectively. Before spectroscopic measurements, the solution was freshly prepared by diluting the high concentration the stock solution to the required concentration. All of the experiments were conducted at standard barometric pressure and room temperature.

Determination of the detection limit

The linear relationship between the fluorescence intensity at 624 nm and the

concentration of NADH was fitted based on the fluorescence titration. The detection limit was calculated using the following equation based on the fluorescence titration[S1].

Detection limit = 3σ/k

Where σ is the standard deviation of the blank sample, k is the slope of the linear regression equation.

Detection of fluorescence quantum yield

A certain volume of the probe is separately added to a different solvent to prepare a solution of a certain concentration. The absorption intensity of the analyte at the excitation wavelength was kept to be less than 0.05, and then its fluorescence emission spectrum was collected. According to the literature, fluorescence quantum yield (Φ_1) was determined by using rhodamine B (Φ_B = 0.71, in ethanol) as the fluorescence standard.[S2] The quantum yield was calculated using the following equation.

$$\Phi_1 = \Phi_B \cdot (A_B/A_1) \cdot (F_1/F_B) \cdot (\lambda_B/\lambda_1) \cdot (\eta_1/\eta_B) \ (A \leq 0.05)$$

Among them, the corner markers 1 and B represent the sample to be tested and the standard, respectively. Φ is the fluorescence quantum yield, A is the absorption intensity at the excitation wavelength, F is the corresponding fluorescence integral area, λ is the excitation wavelength and η is the refractive index of the solvent (Refractive index: water, 1.333; ethanol, 1.362).

Confocal imaging

The cultured HeLa cells were seeded on 24 well chambered cover glass at a density of 1×10^6 cells mL^{-1} for 24 h. Probe dissolved in DMSO were added to the cells medium (500 μL) at a varying final concentrations according to the need. After the probe and cells were incubated for 30 min, the excess probe was gently washed three times with phosphate buffered saline (PBS, pH = 7.4). Fluorescence images were collected by sequentially line scanning with an Olympus FV1000 confocal laser-scanning microscope. Probe was excited at 559 nm and their red emissions were collected in the range of 582-682 nm.

Synthesis and Characterizations

The preparation of 2-[2-methyl-6-(2-quinolin-3-yl-vinyl)-pyran-4-ylidene] malononitrile (DPMQ1).

2, 6-(Dimethyl-4H-pyran-4-ylidene) malononitrile **DPM** (100 mg, 0.58 mmol) and quinolone-3-carboxaldehyde (91 mg, 0.58 mmol) were combined in dry CH_3CN (5.0 mL) in a 50 mL round-bottomed flask, and then piperidine (3 drops) was added. The reaction mixture was stirred at 60 ^oC overnight. After cooling to room temperature, the precipitated was filtered to give the crude product. Finally, the crude product was purified by silica gel column chromatography (SiO_2, CH_2Cl_2/EtOAc, gradient) to obtain a yellow solid **DPMQ1** in 45.5% yield (82 mg); m.p. 280-281 ^oC. HRMS: m/z $[M + H]^+$ = 312.1137; Calcd for $[M + H]^+$: 312.1147; ^1H NMR (DMSO-d_6, 400 MHz, ppm): 2.48 (s, 3H, -CH_3)，6.71 (d, *J* = 2.0 Hz, 1H), 6.92 (d, *J* = 2.0 Hz, 1H), 7.63 (t, *J* = 8.4 Hz, 1H), 7.66 (d, *J*= 12.0 Hz, 1H), 7.69 (d, *J*= 12.0 Hz, 1H), 7.80 (t, *J* = 8.0 Hz, 1H), 7.97 (d, *J* = 8.4 Hz, 1H), 8.04 (d, *J* = 8.4 Hz, 1H), 8.62 (d, *J* = 2.0 Hz, 1H), 9.24 (d, *J* = 2.0 Hz, 1H); ^{13}C NMR (100 MHz, DMSO-d_6, ppm): 19.9, 106.5, 108.2, 108.3, 115.8, 121.4, 121.5, 127.9, 128.0, 128.6, 129.1, 129.3, 131.1, 134.6, 135.6, 135.6, 148.1, 150.0, 157.2, 159.7.

The preparation of DPMQL1.

To a solution of **DPMQ1** (60 mg, 0.19 mmol) in dry CH_3CN (3 mL) in a 25 mL round-bottomed flask, CH_3I (200 μL) and K_2CO_3 (53.3 mg, 0.39 mmol) were successively added. The flask was sealed with a rubber stopper, and then the mixture was stirred at 60 ^oC overnight. After completion of the reaction, excess KBF_4 (120 mg, 0.95 mmol) was added and stirred at room temperature for ca. 2 h. Subsequently, the solvent was evaporated under reduced pressure. The residue was passed through celite and the obtained solid was washed repeatedly with diethyl ether (3 × 5 mL) to obtain a red solid **DPMQL1** in 30% yield (23.2 mg); m.p. 235-236 ^oC. HRMS: m/z $[M - BF_4^-]^+$ = 326.1293; Calcd for $[M - BF_4^-]^+$: 326.1245; ^1H NMR (DMSO-d_6, 400 MHz, ppm): 2.49 (s, 3H, -CH_3), 4.64 (s, 3H, N-CH_3), 6.82 (d, *J*= 1.6 Hz, 1H), 6.92 (d, *J*= 1.6 Hz, 1H), 7.73 (d, *J*= 16.4 Hz, 1H), 7.78 (d, *J*= 16.4 Hz, 1H), 8.08 (t, *J*= 8.0 Hz, 1H), 8.29 (t, *J*= 8.0 Hz, 1H), 8.40 (d, *J*= 8.0 Hz, 1H), 8.52 (d, *J*= 8.0 Hz, 1H), 9.49 (s, 1H), 9.92 (s, 1H); ^{13}C NMR (100 MHz, DMSO-d6, ppm): 19.9, 46.3, 53.3, 58.1,

106.8, 109.4, 115.6, 119.8, 124.7, 129.4, 129.5, 130.9, 131.1, 131.2, 136.4, 138.2, 144.2, 150.4, 156.9, 158.5, 164.9.

Cell viability assay

To analyze percentage of HeLa cell death, MTT assay was performed after drugs treatments. 10000 cells were seeded onto 96 well tissue culture plates in sterile conditions. After harvesting for overnight cells were incubated for 24 h in the absence or presence of 6 different concentrations (0.5 μM, 1 μM, 3 μM, 5 μM, 10 μM, 50 μM) of **DPMQL1**. In addition, we also set up a blank control group and a positive control group (50 μM H_2O_2). Treated cells were incubated for 4 h in presence of MTT solution prepared from 5 mg/mL of 3-(4, 5-dimethyl-thiazol-2-yl)-2, 5-diphenyltetrazolium bromide in PBS. After 4 h incubation, cells were treated with 100 μL DMSO at 37 ºC for 1 h, and then the OD630 data for each well were recorded on PL-9602. Data analysis was performed using following formula:

% of Viable cells = $[(A_{TC} – A_B) / (A_{UC} – A_B)] \times 100$

(TC – Treated cells, B – Background, UC – untreated cells)

To analyze percentage of PC12 cell viability, CCK-8 assay was performed after drugs treatments. 10000 cells were seeded onto 96 well tissue culture plates in sterile conditions. After harvesting for overnight cells were incubated for 24 h in the absence or presence of 6 different concentrations (0.5 μM, 1 μM, 3 μM, 5 μM, 10 μM, 50 μM) of DPMQL1. In addition, we also set up a blank control group and a positive control group (50 μM H2O2). Treated cells were incubated for 1h in presence of CCK-8 solution (10 μL) at 37 ºC. Data analysis was performed using following formula:

% of Viable cells = $[(A_{TC} – A_B) / (A_{UC} – A_B)] \times 100$

(TC – Treated cells, B – Background, UC – untreated cells)

Probe recognition mechanism

The proposed optical responses of the probe DPMQL1 towards NADH were shown in Scheme 3. Before reduced by NADH, both the malononitrile moiety and the chinolinium moiety in DPMQL1 are highly electron-deficient. The intramolecular “push-pull” electronic effect is not obvious. Thus, the probe showed an electron absorption and a weak fluorescence emission at a relative short wavelength region. After reaction with NADH, the chinolinium moiety was reduced, and converted to electron-rich donor. Accordingly, the vinyl bridged electron-deficient malononitrile

moiety and the electron-rich hydrogenated *N*-methylquinoline moiety composed a "push-pull" electronic system in DPMQL-H. Therefore, the electron absorption and a weak fluorescence emission spectra of DPMQL-H were prominently enhanced due to the strong intramolecular charge transfer (ICT).

In order to verify sensing mechanism of probe for NADH, the probe and the product of DPMQL1 with NADH were analyzed by ^{1}H NMR spectroscopy, HRMS and HPLC analysis. The reaction product, DPMQL-H, was observable by its [M + H] signal at m/z 328.1461 (Fig.S7). From the ^{1}H NMR analysis, after the reaction of DPMQL1 with NADH, the N-CH_3 protons of DPMQL1 upfield shifted from 4.68 to 3.54 ppm, and a new singlet at 3.87 ppm emerged (Fig. S8). For HLPC analysis, after the reaction of DPMQL1 with NADH, a new peak at 7.36 min belonging to the reaction product (DPMQL-H) was observed, and the peak at 3.65 min and 2.55 min, corresponding to DPMQL1 and NADH, decreased remarkably (Fig. S9). These data confirmed our proposed recognition mechanism.

To better understand the photochemical properties of **DPMQL1** and **DPMQL-H**, density functional theory (DFT) calculation were carried out by a suite of Gaussian 09 programs (B3LYP/6-31G (d) basis sets). As shown in Fig. S4b, the optimized structures in the ground states of **DPMQL1** and **DPMQL-H** showed that π-conjugated donor-acceptor system of **DPMQL1-H** had a larger conjugated backbone than π-conjugated electron acceptor-acceptor system of **DPMQL1**. The conjugated backbone in **DPMQL1** was partially interrupted by an aromatic ring, while the electronic delocalization of the **DPMQL-H** was changed by hydrogen ion through the internal charge transfer, forming the larger π-extended conjugation. Furthermore, the calculated transition energy ΔE of **DPMQL1** and **DPMQL-H** were 1.68 eV and 0.60 eV (Table S1), respectively. Thus, it led to the enhancement of spectral intensity and red shift in both UV-Vis and fluorescence spectra, and the calculations were consistent with the experimental results.

Table S1 Calculated LUMO and HOMO distributions of **DPMQL1** and **DPMQL1-H**

	LUMO	HOMO	ΔE
DPMQL1	-6.56 eV	-8.24 eV	1.68 eV
DPMQL1-H	-5.18 eV	-5.78 eV	0.60 eV

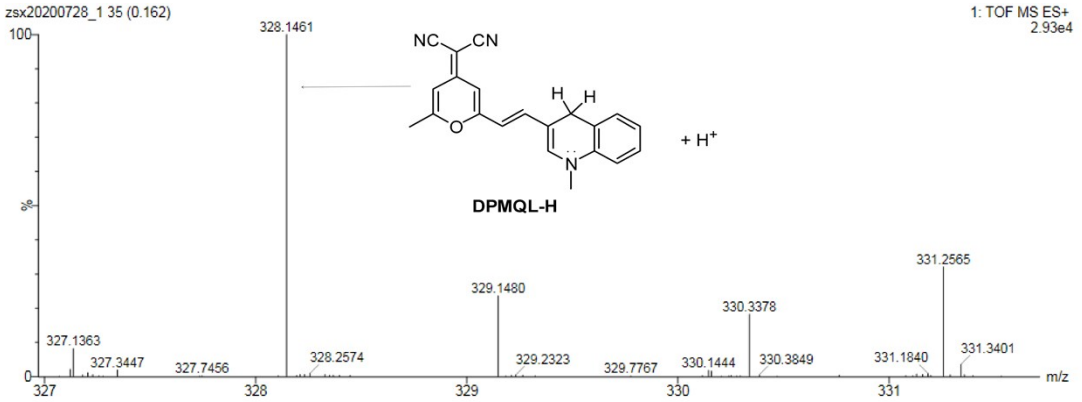

Fig. S1 HRMS spectra of the reaction product of **DPMQL1** with NADH. The peak at m/z = 328.1461was assigned to the mass of [**DPMQL-H** + **H**$^+$].

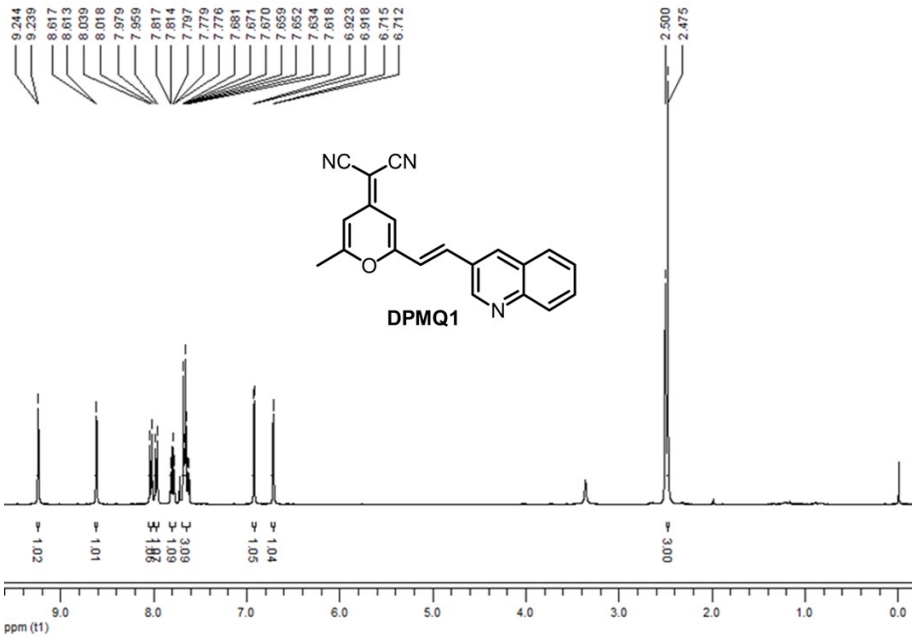

Fig. S2 ^{1}H NMR of **DPMQ1** (400 MHz, DMSO-d_6).

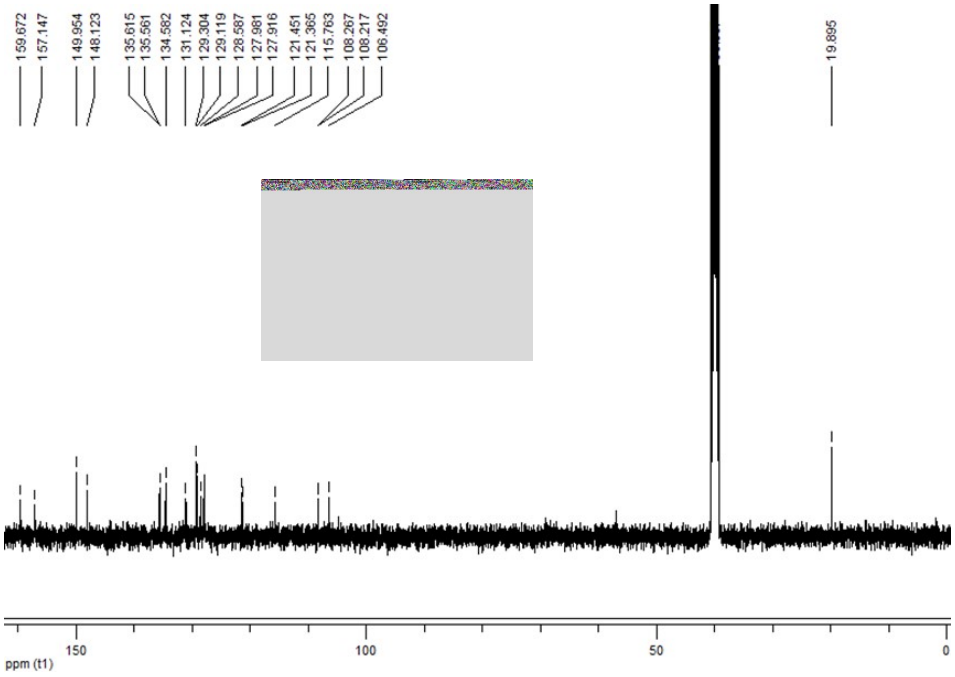

Fig. S3 ^{13}C NMR ^{1}H NMR of **DPMQ1** (100 MHz, DMSO-d_6).

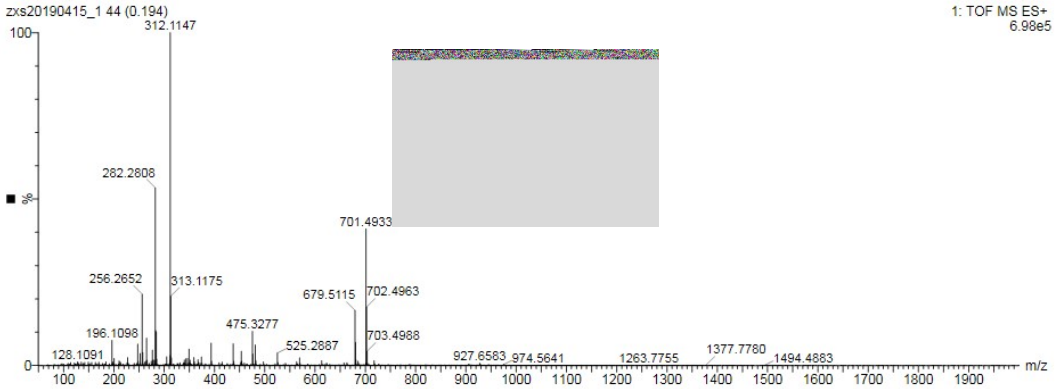

Fig. S4 HRMS (LC/MS) spectra of DPMQ1. The peak at m/z = 312.1147 was assigned to the mass of [**DPMQ1** + H]$^{+}$.

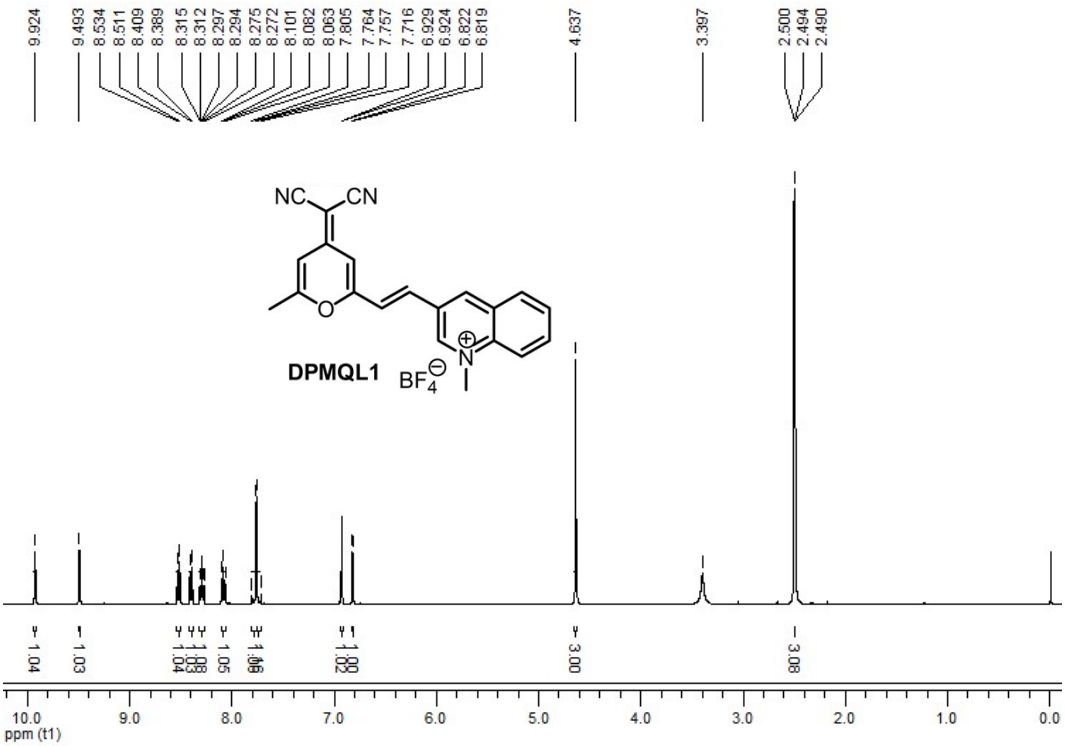

Fig. S5 ^{1}H NMR of **DPMQL1** (400 MHz, DMSO-d_6).

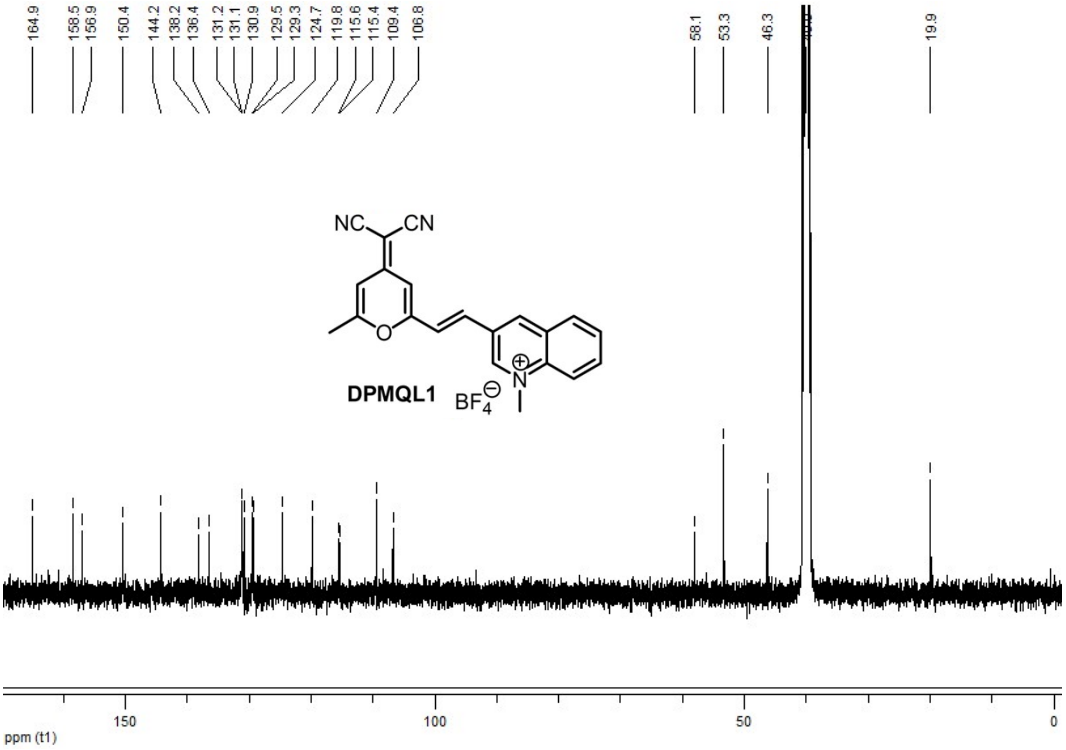

Fig. S6 ^{13}C NMR of **DPMQL1** (100 MHz, DMSO-d_6).

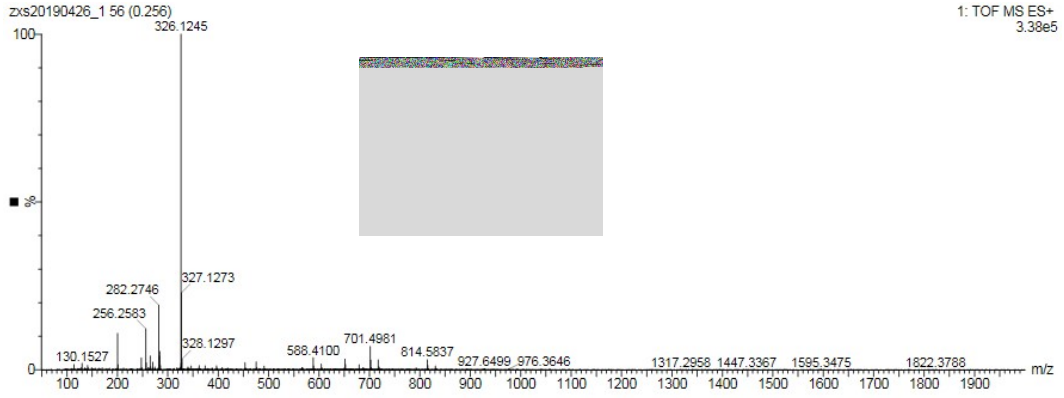

Fig. S7 HRMS (LC/MS) spectra of **DPMQL1**. The peak at m/z = 326.1245 [$(M_{\mathbf{DPMQL1}} - BF_4^-)^+$] was assigned to the mass of **DPMQL1**.

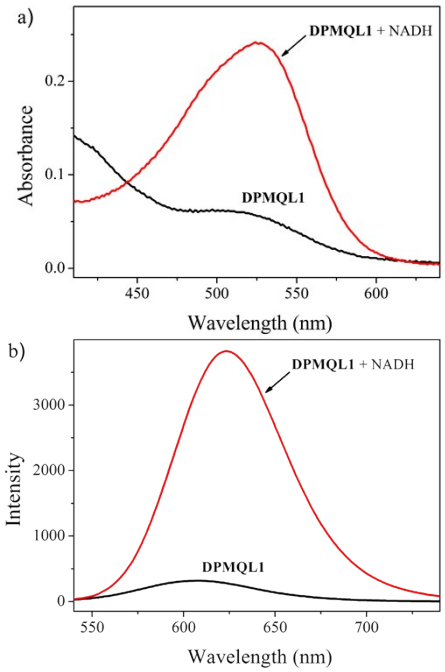

Fig. S8 Absorption a) and fluorescence emission spectra b) of **DPMQL1** in PBS-EtOH (PBS, 10 mM, pH = 7.4, 1: 1, v/v) before and after the addition of NADH. λ_{ex}: 510 nm, slit: 5 nm.

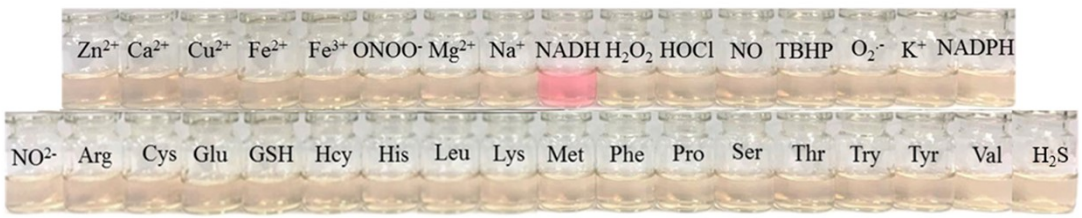

Fig. S9 The change of solution colour of **DPMQL1** (10 μM) in PBS-EtOH (PBS, 10 mM, pH =

7.4, 1: 1, v/v) after joining the various biological species (100 μM). 1-34: Zn^{2+}, Ca^{2+}, Cu^{2+}, Fe^{2+}, Fe^{3+}, K^{+}, Mg^{2+}, Na^{+}, H_2O_2, HOCl, NADH, NADPH, NO, NO_2^{-}, $O_2^{\bullet-}$, $ONOO^{-}$, TBHP, Arg, Cys, Glu, GSH, Hcy, His, Leu, Lys, Met, Phe, Pro, Ser, Thr, Try, Tyr, Val, H_2S.

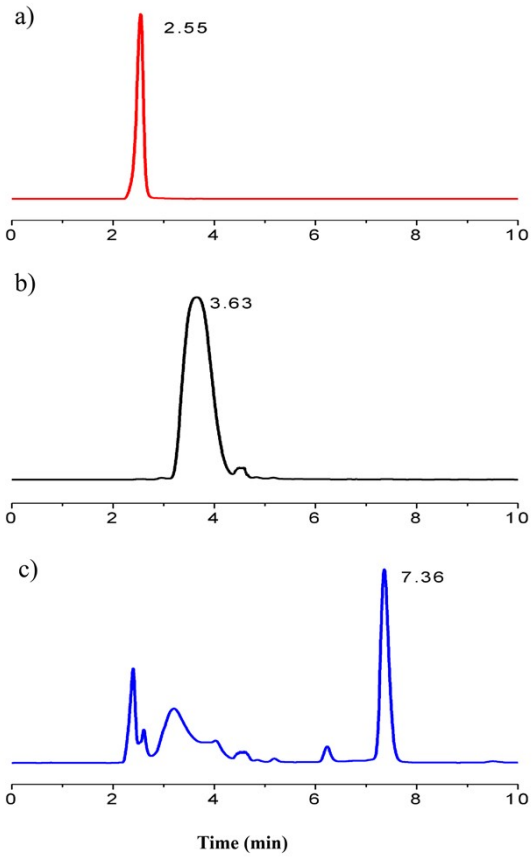

Fig. S10 HPLC profiles of a) 50 μM **NADH** , b) 10 μM **DPMQL1**, c) 50 μM **DPMQL1** mixed with 20 μM NADH. Detection: UV-Vis (365 nm) detector. Flow rate: 1 mL/min. Injection volume: 10 μL. Mobile phase: methanol-water, 80:20 (v/v).

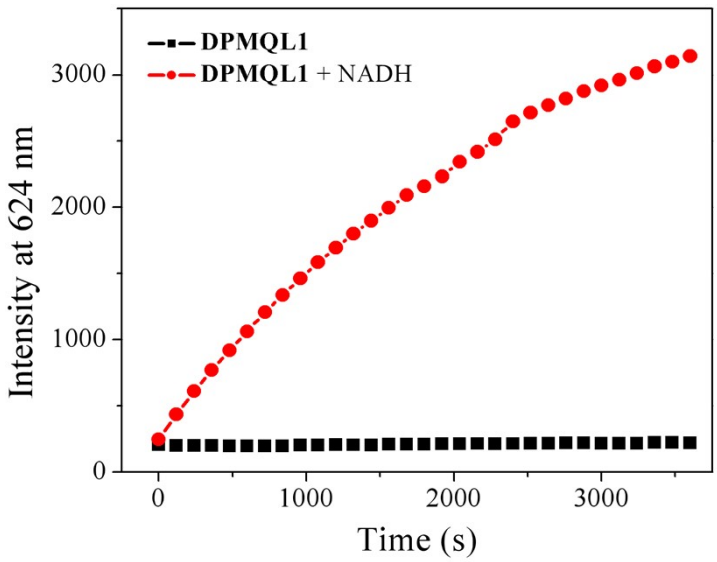

Fig. S11 The fluorescence intensity of **DPMQL1** (5 μM) at 624 nm in the presence of NADH (50 μM) as a function of incubation time. λ_{ex} = 510 nm, slit: 5 nm.

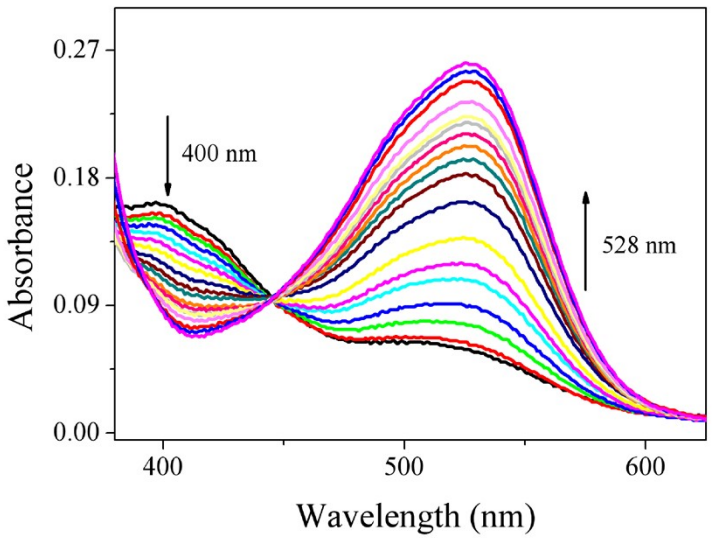

Fig. S12 Absorption spectra of **DPMQL1** (10 μM) with different concentrations of NADH in PBS-EtOH (PBS, 10 mM, pH = 7.4, 1: 1, v/v).

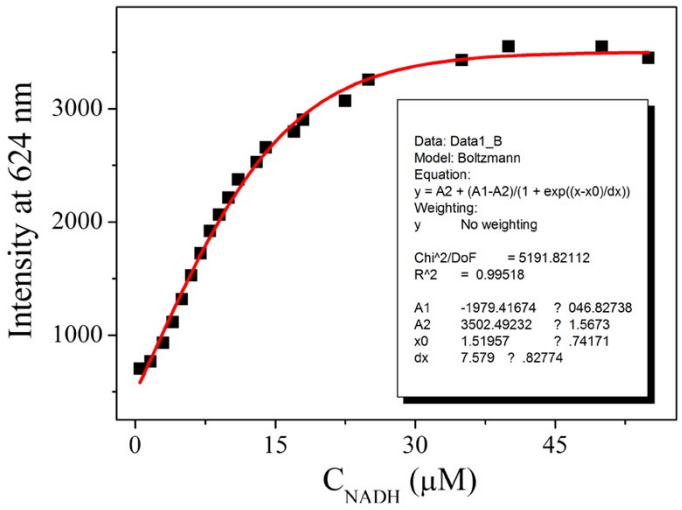

Fig. S13 The fluorescence $K_{turn\text{-}on}$ of **DPMQL1** (5 μM) in PBS-EtOH (PBS, 10 mM, pH = 7.4, 1: 1, v/v) by fluorescent titration experiment. The fluorescent intensity data at 624 nm were fit above nonlinear plot by Origin 7.0 software to give the $K_{turn\text{-}on}$ value. λ_{ex} = 510 nm, slit: 5 nm.

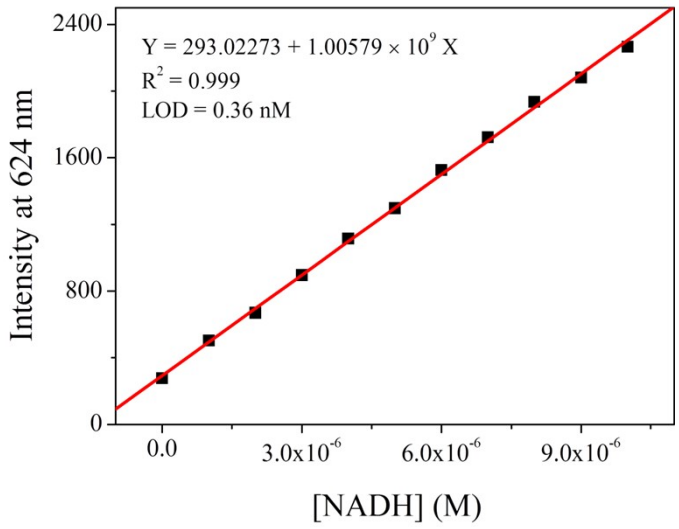

Fig. S14 Detection limits of **DPMQL1** (5 μM) in PBS-EtOH (PBS, 10 mM, pH = 7.4, 1: 1, v/v) by fluorescent titration experiment. The limit of detection (LOD) can be calculated with the equation, LOD = 3σ/k, where "k" is the sensitivity of the fluorescence intensity at 624 nm versus [NADH], and "σ" is the standard deviation of the blank signal (F_0) obtained without NADH ($\sigma_{\mathbf{DPMQL1}}$ = 0.1223). LOD for NADH was calculated to be 0.36 nM under the testing conditions. λ_{ex} = 510 nm, slit: 5 nm.

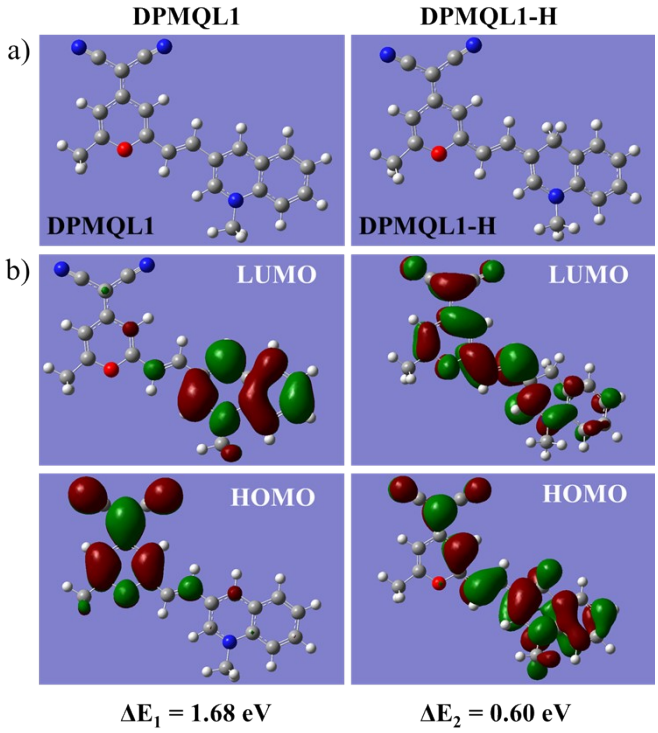

Fig. S15 a) The optimized structure of **DPMQL1** and **DPMQL1-H**; b) DFT optimized frontier orbital pictures of **DPMQL1** and **DPMQL1-H**.

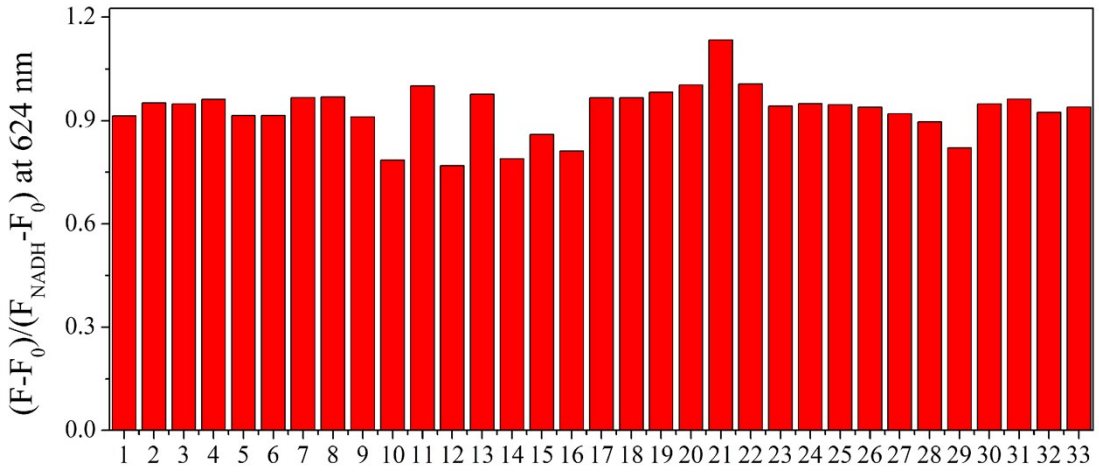

Fig. S16 Fluorescence intensity change ratio $(F-F_0)/(F_{NADH}-F_0)$ of **DPMQL1** (5 μM) at 624 nm towards NADH (50 μM) in the presence of other relevant analytics (50 μM) in PBS-EtOH (PBS, 10 mM, pH = 7.4, 1: 1, v/v). 1: **DPMQL1** + NADH + Zn^{2+}, 2: **DPMQL1** + NADH + Ca^{2+}, 3:

DPMQL1 + NADH + Cu^{2+}, 4: **DPMQL1** + NADH + Fe^{2+}, 5: **DPMQL1** + NADH + Fe^{3+}, 6: **DPMQL1** + NADH + K^{+}, 7: **DPMQL1** + NADH + Mg^{2+}, 8: **DPMQL1** + NADH + Na^{+}, 9: **DPMQL1** + NADH + H_2O_2, 10: **DPMQL1** + NADH + HOCl, 11: **DPMQL1** + NADH + NADH, 12: **DPMQL1** + NADH + NAD(P)H, 13: **DPMQL1** + NADH + NO, 14: **DPMQL1** + NADH + NO_2^{-}, 15: **DPMQL1** + NADH + $O_2^{\bullet -}$,16: **DPMQL1** + NADH + $ONOO^{-}$, 17: **DPMQL1** + NADH + TBHP, 18: **DPMQL1** + NADH + Arg, 19: **DPMQL1** + NADH + Cys, 20: **DPMQL1** + NADH + Glu, 21: **DPMQL1** + NADH + GSH, 22: **DPMQL1** + NADH + Hcy, 23: **DPMQL1** + NADH + His, 24: **DPMQL1** + NADH + Leu, 25: **DPMQL1** + NADH + Lys, 26: **DPMQL1** + NADH + Met, 27: **DPMQL1** + NADH + Phe, 28: **DPMQL1** + NADH + Pro, 29: **DPMQL1** + NADH + Ser, 30: **DPMQL1** + NADH + Thr, 31: **DPMQL1** + NADH + Try, 32: **DPMQL1** + NADH + Tyr, 33: **DPMQL1** + NADH + Val; λ_{ex} = 510 nm, slit: 5 nm.

Reference

[S1] Y. Lu, S. S. Huang, Y. Y. Liu, S. He, L. C. Zhao, X. S. Zeng, Org. Lett. 13 (2011) 5274-5277.

[S2] D. Oushiki, H. Kojima, T. Terai, M. Arita, K. Hanaoka, Y. Urano, J. Am. Chem. Soc. 132 (2010) 2795-2801.